JOURNAL OF MATERIALS SCIENCE **39** (2004) 3877–3887

Looking into details of atom kinetics in intermetallics

W. PFEILER, W. PÜSCHL
Institut für Materialphysik, University of Vienna, Strudlhofgasse 4, A-1090 Vienna, Austria
E-mail: pfeiler@ap.univie.ac.at

R. PODLOUCKY
Center for Computational Materials Science and Institut für Physikalische Chemie, University of Vienna, Liechtensteinstrasse 22a/l/3, A-1090 Vienna, Austria

Information on the atom jump processes during the establishment and destruction of long-range order can be gained from measurement of residual electrical resistivity (REST). By its nature this very sensitive method yields an integral signal, so theoretical efforts are mandatory to properly understand how the single atom jumps work together in generating it. As a valuable approach we report on Monte Carlo simulations of atom kinetics which process the individual jumps into macroscopic configurational changes. In order to create a more reliable quantitative basis for individual jump frequencies we propose *ab initio* calculations of defect energies and migration profiles, a method which has become increasingly accessible in recent years. When experimental investigation is enlightened by combining these two theoretical methods, we expect deep insight into the hierarchy of atomic movement during changes of the ordered state. First steps towards such an ideal program are discussed. An outlook is given how the theoretical methods described offer structural and kinetic information on various scales and in different systems.

1. Introduction

Intermetallics have been one of the foremost topics in materials science for years due to their technical application as high-temperature structural materials [1, 2]. Recently some of these compounds have been proposed as magnetic or magneto-optical high-density information storage media [3, 4] and novel high-temperature actuators [5, 6]. The basis for all projects aiming at the design of innovative materials for future high-performance technical applications is a thorough knowledge of the atomistic processes determining structural changes and stability. Many of the desired properties of intermetallics are intimately linked to a high degree of chemical long-range order (LRO). It is therefore very important to understand the atom jump processes leading to changes of order.

How can details of the atomic movement be observed in intermetallic alloys? Usual diffusion experiments e.g., by measuring tracer diffusivity [7, 8] or as recently by using a SIMS (secondary ion mass spectroscopy) analysis of the diffusion of a corresponding stable isotope [9, 10] give information on atom jumps during long-range diffusion keeping constant on average the degree of LRO ('steady state diffusion'). The same holds for the observation of the atomic jump vector by various scattering methods under equilibrium conditions [11, 12].

A completely different approach concerns so-called 'order-order' relaxation experiments [13, 14]. In this case, the system under observation is slightly pushed out of its thermodynamical equilibrium state at a constant temperature by the application of a correspondingly small temperature shift, and the subsequent relaxation into a new thermodynamic equilibrium is carefully observed. During such order relaxation experiments just those atom jumps are observed which enable a *change* in the degree of LRO. In this way the processes can be studied which are liable to destroy thermodynamic stability of the intermetallics and their corresponding advantageous mechanical high-temperature properties.

Interestingly, there is up to now only one experimental method with the necessary high precision so that the very small changes of the degree of order which correspond to slight changes of temperature can be resolved. This is the measurement of residual resistometry (REST) which is known for its ultra-high sensitivity for structural changes [15]. More details about this interesting method will be given in the next section.

REST measurements yield an integral signal composed of several effects, and considerable experience is necessary to separate them correctly. We are of course interested to interpret the macroscopic kinetics in the light of what is happening at the atomic scale. What is needed is firstly as detailed information as possible on the single atom jump in different environments, secondly a method to sum up the individual atom jumps statistically and therefore arrive

at the mesoscopic/macroscopic kinetic behaviour. The latter task can be fulfilled by kinetic Monte Carlo (MC) algorithms. Section 3 of this paper is dedicated to a discussion of how to apply MC simulations in the study of ordering/disordering kinetics in intermetallics, together with the limitations and problems that have to be taken care of.

Striving to obtain a valid description of the single atomic jump process we cannot ignore that quantum-mechanical first principles calculation of materials parameters have become more and more accurate in recent years in parallel with the exponentially increasing computing capacity. Reliable defect formation energies for antisite atoms or vacancies on the different sublattices can be determined with an error margin below 0.1 eV. The energy profile encountered by a migrating atom can be obtained by quasi-static displacement of the atom, relaxing the neigbourhood atoms at each step. A molecular dynamics simulation would yield additional information on effects of motion. It is necessary, however, to find suitable potentials for the interacting atoms considered. In view of the excellent tools available, it is altogether imperative to do some first-principles calculations of crystal defect properties in intermetallics, especially of those which mediate atom jumps and atomic diffusion. In Section 4 therefore modern methods are shortly sketched and it is shown how properties like defect formation and migration enthalpies and migration profiles can be calculated directly.

It can be hoped that combining crystal defect properties as calculated by *ab initio* methods with advanced *kinetic* MC simulation methods and comparing the results to the experiments of 'order-order' relaxations by REST will give a deep insight into the atom kinetics in intermetallic alloys.

2. Study of atom jumps in intermetallics by investigating 'order-order' relaxations

The study of ordering kinetics during an order-disorder transformation has been in the focus of research in alloy physics and materials science for several years. The formation of the LRO state from a disordered solid solution is of course a complex phenomenon involving several mechanisms which occur simultaneously [16] and depends on the actual phase transition, first order or higher order. This complexity concerns theoretical considerations but even more experimental studies, because the individual processes cannot easily be separated from each other.

A way out of this problem is to first generate a highly ordered state in the sample and then to study fine variations of the degree of LRO, so-called 'order-order' relaxations. In this case after equilibrating the system at a certain degree of order, it is suddenly pushed out of its equilibrium state, for example by changing abruptly the annealing temperature by a small amount. Subsequently the relaxation into the new equilibrium state which corresponds to the new annealing temperature is recorded.

It is obvious that in highly ordered intermetallics the variation of the order parameter following a sudden temperature change of only 10–20 K is minute, that is in the order of magnitude of 0.1% or less. At present, the only experimental method with a resolution high enough for these extremely small changes of LRO is that of residual resistometry (REST). In this method of resistivity measurement the measuring procedure is done at low temperatures such as liquid nitrogen or liquid helium temperature and separated from the annealing treatment at sufficiently high temperature as necessary to establish a thermodynamical equilibrium of the atomic distribution. The current state of the sample after each annealing treatment is frozen in by a fast quench to the low (and constant) measuring temperature. This way the phonon contribution is kept constant and very small so that an ultra-high accuracy is achieved (resolution of about 10^{-5} for changes in LRO parameter well below the order/disorder transition temperature).

Electrical resistivity is affected by changes of LRO due to diffuse scattering of conduction electrons and in addition by superlattice Bragg scattering, which changes the effective density of conduction electrons. Using an appropriate pseudopotential formalism for the electron scattering and considering the change in the effective density of conduction electrons in an approximate way by comparing with magnetic systems, Rossiter [17] arrived at a comparatively simple dependence for the temperature independent part of resistivity on the degree of homogeneous LRO:

$$\rho_{\mathrm{LRO}}/\rho_{\mathrm{D}} = (1-\eta^2)/(1-A\cdot\eta^2). \qquad (1)$$

η is the LRO-parameter, the coefficient A (used as a single fit parameter when calculating η directly from resistivity measurement) depends upon the relative positions of the Fermi surface and the superlattice Brillouin zone boundaries. Equation 1 is of astonishing validity as recently checked by parallel measurements of resistivity and X-ray scattering [18, 19]. There is still missing, however, a more rigorous approach to LRO-resistivity which considers realistic band structures and takes into account deviations from homogeneity in a structure containing antiphase boundaries.

Whereas a description of the experimental method in full length is given in several original papers the value of these experiments will be explained here by means of some selected examples. As a first example a small-step annealing treatment on equiatomic FePd is shown in Fig. 1. FePd belongs to a subgroup of intermetallics which due to their $L1_0$-ordering display a marked mechanical and magnetic anisotropy. This is the reason why they recently became technically interesting as high density data storage media [3, 4]. Since the anisotropy is strictly linked to a high degree of LRO, it is of course of vital importance to study the atomic jump processes which lead to changes of the degree of LRO. The REST measurements of Fig. 1 reflect changes of LRO during order-order relaxations. From the behaviour of the relaxation curves it can be decided that the same final plateau values are achieved for up-steps and down-steps to the same annealing temperature (stable equilibrium values). A kinetic analysis of

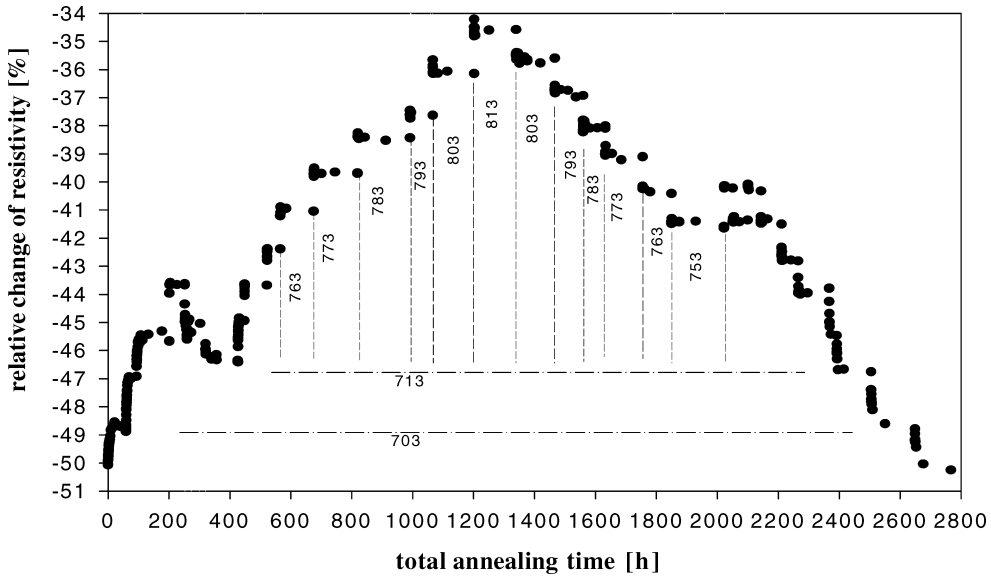

Figure 1 Small-step annealing treatment of FePd to study 'order-order' relaxations between definite states of LRO [20]. Some corresponding annealing temperatures are indicated.

the individual relaxation curves yields relaxation times corresponding to the involved processes which can be compiled in an Arrhenius-plot leading to activation energies [20].

As a further example of the advantages of REST in Fig. 2 the change of resistivity of Cu_3Au as a function of annealing time during disorder-order measurements is compared with 'small-step' annealing treatments (order-order relaxation) [19]. Of two samples relaxed during annealing one is repeatedly disordered after each annealing (full symbols) whereas the other sample always remains in its increasingly ordered state (open symbols, for more details see [19]). It can be seen from Fig. 2 that the kinetic behaviour results different for the disordered and the ordered sample, respectively. A careful analysis showed that for the disorder-order transformation besides a fast ordering process describing the order-order relaxations by a fast elimination of antisite atoms within the well-developed ordered domains, a very slow process is involved which could be explained as arising from the growth of ordered domains: As antiphase boundaries dissolve, the overall

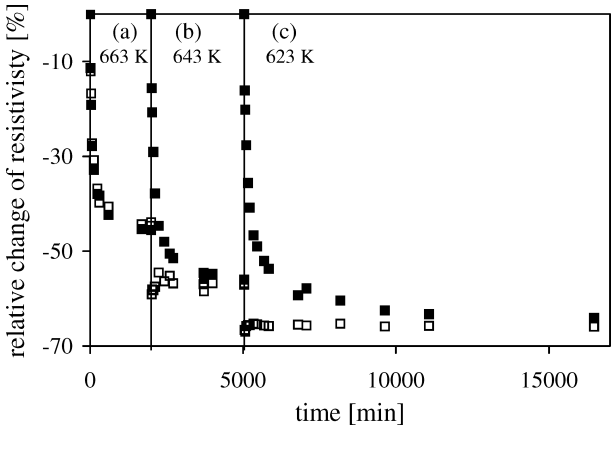

Figure 2 Relative change of resistivity during isothermal annealing of Cu_3Au. For details see text and [19].

LRO-parameter increases. This example demonstrates that the evolution of the antiphase structure yields a considerable contribution to electrical resistivity which under certain circumstances can be separated from the homogeneous LRO-resistivity.

A third example for the efficiency of the REST-method demonstrates how the high resolution can elucidate the phenomena during the very early states of LRO-establishment. A detailed investigation of changes of LRO in B2-ordered Fe-48 at.% Al by REST brought to light an unexpected behaviour [21]. Keeping to low annealing temperatures and/or short annealing times quasi-stable states of LRO were observed in considerable distance from values of thermodynamical equilibrium. With increasing temperatures and/or increasing annealing times a growing tendency towards true states of thermodynamic equilibrium became apparent. The findings could be consistently explained by the temperature/time-dependent action of the vacancies which mediate all configurational changes in a material like FeAl. This is demonstrated in Fig. 3, where the change of resistivity during isochronal annealing is given as a function of the annealing temperature. The increasing volume of the sample the vacancies visit with increasing temperature and time during their random walk is demonstrated by a 2D numerical simulation of the vacancy motion and given by inserts at the corresponding annealing temperatures. Regions of the crystal that have been visited by a vacancy appear in black. It is seen from this qualitative illustration that an overall thermodynamic equilibrium of order in the whole crystal volume is achieved only when these regions become interconnected. It can be concluded that the experimental observation of vacancy-mediated changes of atomic configurations for certain vacancy parameters will yield different results in different temperature intervals [22]. What this really means is: The diffusion mediating defect mechanism may *change completely* the original transformation process as expected from a continuum kinetic treatment.

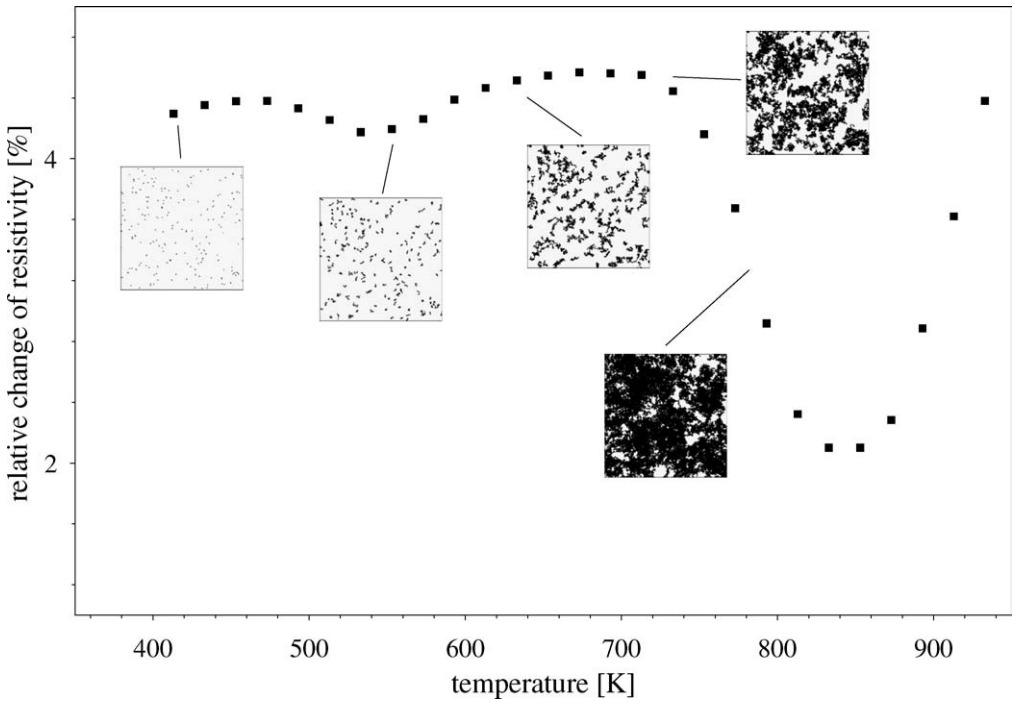

Figure 3 Relative change of resistivity versus temperature as measured during isochronal annealing of Fe-44.8 at.%Al [21]. The inserts for some given temperatures schematically show the regions which have been visited by vacancies during their random walk within the isochronal time interval (black).

A final example has to be mentioned with respect to the proposed comparison with MC simulations of atom movement and *ab initio* calculations of defect properties. $Ni_{76}Al_{24}$ + 0.19 at.%B was investigated by REST during a small-step annealing treatment. The analysis of the very fine resistivity changes during the LRO-relaxations gave evidence for the simultaneous action of two processes with a considerable difference in relaxation time and a comparatively high ordering activation energy greater than 4 eV. Experimental details and findings are already very well documented [23, 24]. The puzzling results from experiment stimulated simulation studies of atomic movement as well as the calculation of defect properties from first principles which are shown in the next subsections.

3. Kinetic Monte-Carlo simulation

Many single atom jumps work together to change the configuration of an alloy over a time interval of observation. How can we describe this collective process? Different levels of approximation are obviously possible. In the most far-reaching simplification, we would regard a typical lattice site, say a position on a specified sublattice, surrounded by an average environment determined for instance by the current value of an LRO parameter. A mean flux of atoms/vacancies to or from this lattice site would then induce a change of the occupation probability for a given atom for the site type considered. While such a mean field model leads to an order-disorder kinetics of sorts, it is certainly not able to account for any details resulting from higher-order correlations or to deal with inhomogeneities in order parameter or composition. Reducing by one level the amount of averaging and advancing towards a more general description we arrive at a model where each lattice site is regarded individually [25–27], its occupation probability changing by a net flux of atoms/vacancies depending on its specific surroundings. How these enter the flux equations now depends on the amount of correlations considered and on the averaging procedure chosen. Both this latter type of model, which can describe the evolution of spatially inhomogeneous structures, and the previous one, being master-equation methods, cannot however deal with phase transitions like nucleation where paths contrary to the mean path become rate-determining. Monte Carlo simulations escape this specific limitation by doing a computer experiment mimicking as closely as possible what is actually happening in the real crystal: Atoms move by chance according to a distribution of jump probabilities (see textbook by Binder and Heermann [28]). As the set of lattice sites considered in the simulation cannot be as large as the real specimen, the numerical limitation has to be compensated statistically by repeating the simulation a certain number of times with different random number sequences.

The simplest and historically the first MC simulation method was the Metropolis algorithm, originally employed to calculate the motion of neutrons [29]. The probability of a transition was taken to be a Boltzmann factor containing the difference in internal energy before and after the transition. If the jump resulted in lower energy, it was assumed to happen practically instantly with probability 1. An attempt frequency could be omitted in choosing the time step of the MC simulation as reciprocal to it. Carrying out a normalization so that the probabilities sum up to one we arrive at the

still widely used Glauber algorithm [30]:

$$\Pi_{ij} = \frac{e^{-\frac{\Delta E}{kT}}}{1 + e^{-\frac{\Delta E}{kT}}} \tag{2}$$

It must be noted that this probability is not a pure Boltzmann factor if the denominator in Equation 2 is not close to one, and inconsistencies could be incurred when making an Arrhenius analysis of kinetics as found by MC simulation.

At each MC step, the dice are thrown twice: First potential jump partners are chosen. Then another random number r is generated to decide if a jump takes place at all:

$$\begin{aligned} r &\in [0, 1] \\ 0 \le r \le \Pi_{ij} &\quad \text{jump} \\ \Pi_{ij} < r \le 1 &\quad \text{no jump} \end{aligned} \tag{3}$$

The obvious disadvantage of such a procedure is that if the Boltzmann factor is small, a large number of "empty" cycles could occur. This led to the development of a MC algorithm where a jump is guaranteed at each cycle, the so-called residence time algorithm [31–33] . It is founded on the concept of the diffusion jump as a Markovian process. In the case of a vacancy mechanism, let us regard an ensemble of vacancies each sitting in identical environment amidst z nearest neighbour atoms. Each of these systems can be in state 0, when the vacancy has not yet jumped and is at its original position, or in any of the states j, $j = 1, \ldots, z$, after it has exchanged with atom j. Calling the transition probabilities per unit of time Γ_j, we arrive at the following set of differential equations governing the state of the ensemble (p_0 is the number of systems in state 0, divided by the total number of systems in the ensemble etc.):

$$\begin{aligned} \dot{p}_0 &= -p_0 \sum_{j=1}^{z} \Gamma_j \\ \dot{p}_j &= p_0 \Gamma_j \end{aligned} \tag{4}$$

with solution

$$\begin{aligned} p_0 &= e^{-\sum \Gamma_j t} \\ p_j &= \frac{\Gamma_j}{\sum \Gamma_j}\left[1 - e^{-\sum \Gamma_j t}\right] \end{aligned} \tag{5}$$

It is thus seen that the original state of the vacancy decays with the sum of the transition intensities by exchange with all possible jump partners. The time interval of the MC step is now taken as

$$\Delta t = \frac{1}{\sum \Gamma_j} \tag{6}$$

after which the probability of the original state has decayed by $1/e$. This way it is guaranteed that with reasonable probability at least one of these jumps will have happened within Δt. Of course one has to keep a record of the sum of the intervals which can be translated to physical time with proper assumptions on prefactors and attempt frequency. (A refinement of the algorithm determines the length of Δt by another random variable, after which one proceeds with the solution of the differential Equations 5. This complication does not seem to be worthwhile, however). The decay channel j has now to be determined by a random variable r. The relative probability is

$$q_j = \frac{\Gamma_j}{\sum \Gamma_j} \tag{7}$$

Channel j is chosen, if

$$\begin{aligned} r &\in [0, 1] \\ \sum_{k=1}^{j-1} q_k < r &\le \sum_{k=1}^{j} q_k \end{aligned} \tag{8}$$

The obvious advantage of the residence time algorithm is that empty cycles are avoided, the disadvantage is that probabilities for all of the z possible jumps have to be calculated. This makes this algorithm less suitable for direct exchange of atoms (Kawasaki dynamics) because of the necessary book-keeping for all possible jumps. It is, however, very well suited for a vacancy mechanism. One vacancy in the computation cell suffices, if vacancy concentration is sufficiently small to exclude vacancy-vacancy interaction effects: Because a jump takes place in any case, no (computing) time is won when introducing more vacancies into the calculation.

Up to now we did not give any explicit shape to the transition rates Γ_j. If the lattice is sufficiently stable and gradients and driving forces are not too large, with reasonable confidence we can apply transition state theory [34]. It assumes that as soon as the jumping atom has reached a transition saddle point state which is thought to be in thermal equilibrium with the initial resting state, it will certainly make the transition. For the transition rate we get in this case

$$\Gamma_j = \nu_j e^{-\frac{\Delta E_{is}}{kT}} \tag{9}$$

where ν_j is an attempt frequency containing a quotient of normal frequencies in the initial and the transition state, respectively, and a factor accounting for the difference in vibrational entropy between initial state and transition state. ΔE_{is} means the energy difference between initial and saddle point state, which has to be calculated by means of a sufficiently accurate model of the crystal energy. In some instances it may be approximated by pair interactions broken when the atom is taken from its intial resting position and restored when at the saddle point:

$$\Delta E_{is} = \sum_s \varepsilon'_{is} - \sum_i \varepsilon_{ij} \tag{10}$$

MC simulations of atom configuration equilibria and kinetics were performed almost as soon as electronic

computing became available (see review [35]). From the great number of MC studies we name but a few examples. A direct exchange of atoms was often used in connection with a Metropolis or Glauber-type algorithm because it speeded up the calculation with respect to a vacancy mechanism. For this reason the question arose how the kinetic path was affected by the specific exchange mechanism adopted. It could be shown that a vacancy mechanism and a direct exchange mechanism can lead to significant qualitative and quantitative differences. So it turned out that a considerable amount of antisite defects remain within the ordered domains due to the strong localization of vacancies to the domain boundaries [36], an effect which is not seen with a direct-exchange mechanism. In investigations of short-range ordering, Gahn and Pitsch [37, 38] directly showed the influence of the atom jump mechanism on the kinetic path in a phase space subtendend by different short-range order parameters.

An extensive investigation of ordering kinetics in $L1_2$-ordered Ni_3Al was undertaken by Kozubski and co-workers [39–41] using initially a Glauber-type algorithm. Like the experimental resistivity curves [23, 24], the long-range order parameter could be rendered well by a linear combination of two exponentials. This was later proved in a more direct way by performing, again by MC techniques, what essentially amounts to a Laplace transform. The resulting spectrum of exponential relaxation processes very clearly shows a bimodal distribution [40].

It was the group around G. Martin and P. Bellon who first made extensive use of a residence-time algorithm for atom kinetics via a vacancy mechanism. As a very interesting example of the systems treated by these authors showing at the same time ordering and precipitation we mention B2-ordered FeAl below and in the vicinity of a tricritical point [42]. Depending sensitively on concentration and the exact value of the asymmetry $\varepsilon_{AA}-\varepsilon_{BB}$ in the cohesive energies different complex morphologies appear showing remarkable similarity to experiments [43] (Fig. 4). The phenomenon of localised ordering in the restricted random walk regions of the vacancies could also be observed (compare [22, 44], and chapter 2 of this paper).

Fratzl and co-workers [45, 46] included a term accounting for elastic energy in the Ising-like Hamiltonian of a segregating system and were thus able to reproduce typical shapes of precipitate particles as a consequence of elastic anisotropy. In another simulation [47], it was shown, that the qualitative behaviour of coarsening of a disperse precipitate phase is influenced by the diffusion mechanism. In the direct-exchange model (Kawasaki dynamics) classical Ostwald ripening always predominates, which is based on solute transport between small and large particles by diffusion in the matrix phase. For a vacancy mechanism movement of the whole precipitate and coagulation can become the dominant coarsening mechanism. The obvious reason is that vacancies are attracted to phase boundaries.

Work is in progress with the intention to make the MC computation both more economical and more meaningful from the physical standpoint. As an example we mention the search for shortcuts around strongly correlated jumps which would have the vacancy oscillating for a large number of cycles between two lattice sites [48]. Theoretical improvement must be achieved by finding more well-founded expressions for the transition probabilities. According to transition state theory the initial and the saddle point energies of the jumping atom must be known for the given atomic environment. In many treatments essentially only the initial and final states have been used for the transition probabilities, and only in the approximation of pair interactions. At this point, the *ab initio* efforts come into play.

4. *Ab initio* approach to energetics of lattice defects and their migration barriers

It is our aim to describe interactions between atoms by solving Schrödinger's equation for the wavefunctions of electrons of the many atoms in a solid. The fundamental problem herein is the many-body interaction of the electronic system. Within density functional theory as derived by Hohenberg and Kohn [49] the central rôle of the wavefunction is replaced by the electron density which in a unique way determines the total energy of the ground state of the electrons in the external potential generated by the nuclei.

A major step for *practical application* was done by Kohn and Sham [50] who introduced an effective single-particle orbital like scheme. The purpose of these orbitals is to build up the true ground state charge density which defines—when integrated—the total number of electrons. From these ideas a stationary Schrödinger like equation of the form

$$\hat{H}\Phi_i = \varepsilon_i \Phi_i \tag{11}$$

$$\hat{H} := (-\hbar^2/2m)\Delta + v_{\text{eff}}(\mathbf{r}) \tag{12}$$

for the i-th quantum state is derived. The effective potential $v_{\text{eff}}(\mathbf{r})$ is a sum of the external potential, classical Coulomb interactions plus a term v_{xc} which contains the many-body or exchange-correlation interactions. The quality of the results then depends on the approximations one has to make for the potential v_{xc}. The first and astonishingly successful approximation was based on the homogeneous electron gas: locally the true electron density was replaced by the density value of the electron gas for which the exchange-correlation energy can be determined (local-density approximation, LDA). Leading to significant errors for systems with valence electrons of a more localised nature, LDA was later systematically improved leading to a variety of general-gradient approximations (GGA).

For the treatment of localised defects, Green's function methods have been proposed [51, 52]. However, they cannot be generalized to more complex structures and lattices with reasonable effort. Therefore, for defects in alloys, compounds etc. one rather chooses methods with three-dimensional boundary conditions for which one knows that unit cells with 50–100 atoms can be treated with very good accuracy and reasonable computer time. The defects are then included within a

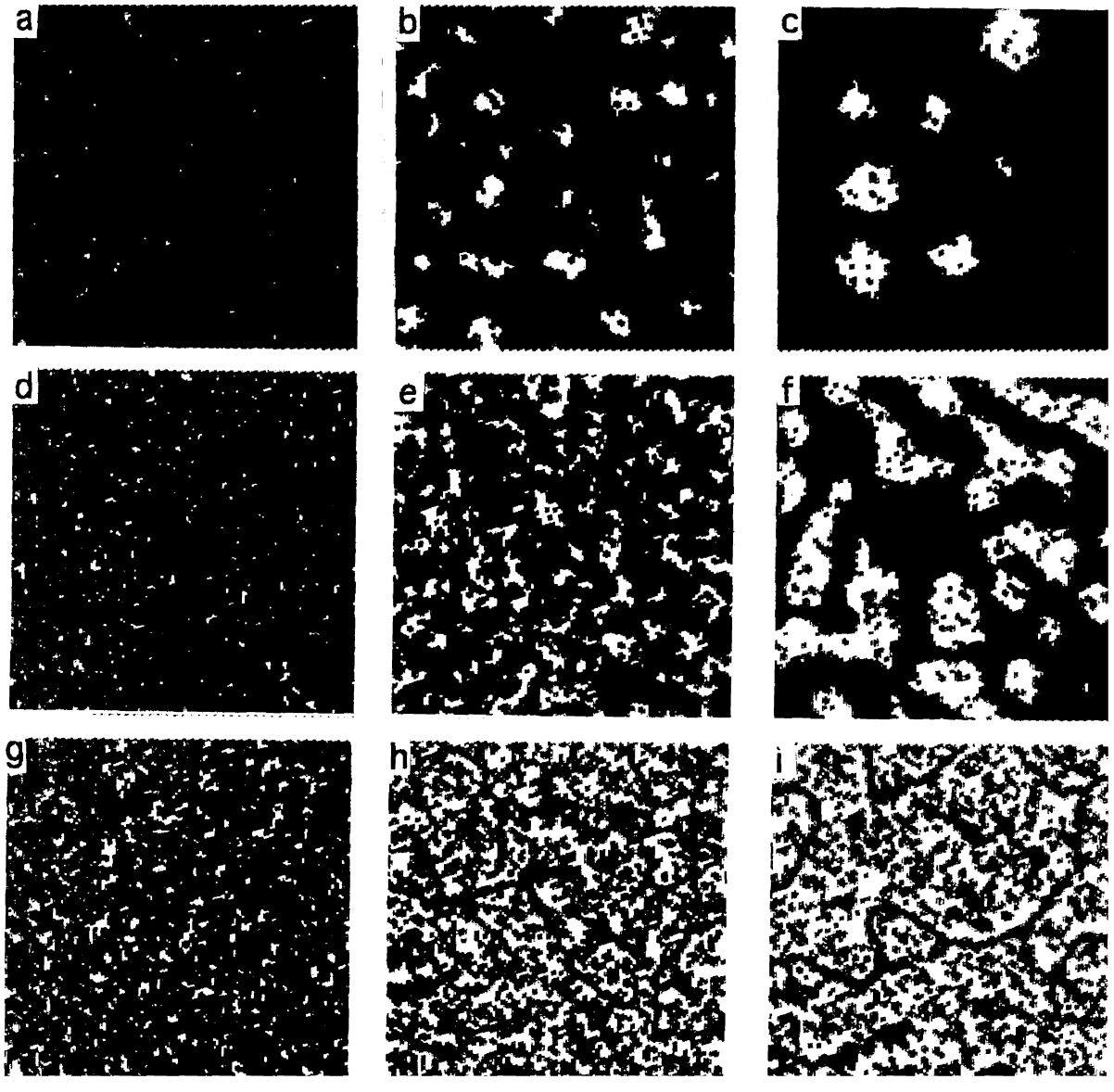

Figure 4 Simulation of ageing sequences (horizontally) in FeAl below the tricritical point [42]. A2 and B2 phases appear as dark and white regions, respectively. Al concentrations are: 10% (a)–(c), 25% (d)–(f), 40% (g)–(i).

suitable supercell. Its size should be sufficiently large so that defect-defect interactions become vanishingly small which can be tested by calculating energies as a function of supercell size. Having accepted the supercell concept, all well-established quantities can then be derived such as forces and energies, and —what is more demanding–reaction and diffusion paths and barriers.

The description of the effective potential must be chosen according to the specific requirements. In particular when accurate forces in a low-symmetry environment are needed, methods without shape approximations to potential or charge density have to be applied. One of the most accurate methods is the all-electron full-potential linearized augmented plane wave (FLAPW) [53] approach. Pseudopotential methods, in which valence electrons move in a field of ions generated by the nuclei and the frozen core charges, are faster in particular for large systems. If the pseudopotential is constructed as close as possible to the true potential—as it is done by the projected-augmented-wave [54] version of the Vienna Simulation Package (VASP) [55]—then the results of VASP and FLAPW are very close as was tested extensively. All results discussed in the following section are based on VASP calculations.

Strictly speaking, energies based on standard density functional theory are valid only for the groundstate at $T = 0$ K. This restriction can, however, be lifted and statistical temperature dependent quantities can be derived as will be discussed below. A physically useful energy always has to refer to some reference. The computational methods deliver either total energies (for all-electron methods) or pseudocohesive energies for pseudopotential type calculations. Only differences of such energies are meaningful, e.g.,

$$\Delta E(N_1, \ldots N_n) = E_{comp}(N_1, \ldots N_n) - [N_1 E_1 + \cdots N_n E_n] \quad (13)$$

The quantity E_{comp} is the calculated energy for a compound consisting of N_i atoms of type i, and E_i are suitable reference energies. For example, the energy of formation for Ni_3Al is calculated by taking the difference of the groundstate energies, $\Delta E(Ni_3Al)$

$= E(Ni_3Al) - [3E(Ni) + E(Al)]$ with the reference energies $E(Ni)$ and $E(Al)$ describing the metallic ground states. Considering the *ab initio* energy $E(V, T = 0)$ as a function of volume V the formation energy ΔE corresponds to a difference of Helmholtz free energies with $T = 0$.

Our aim is to investigate the stability of point-like defects for binary intermetallic compounds such as Ni_3Al. On the basis of density functional results, temperature and concentration dependent formation energies, concentrations of defects and related quantities are calculated in the framework of a statistical model. For the present considerations we focus on the most simple defects which consist in antisite atoms and vacancies on the respective sublattices.

The derivation of a statistical concept for an homogenous compound is more complicated than for one-atom type systems by the condition that stoichiometry has to be preserved which means that various kinds of defects have to coexist. It is necessary to work with a grandcanonical ensemble for which the number of particles can be adjusted by chemical potentials [56, 57].

Let the supercell energy for a defect species A at lattice site λ be ε_A^λ. For example, ε_{Al}^{Ni} denotes an Al antisite defect for which an Al atom is sitting on a site of the Ni sublattice. For a supercell of 32 atomic sites corresponding to the Ni_3Al lattice, the composition with this antisite is $Ni_{23}Al_9$. The supercell energy for a vacancy at the Ni sublattice is given by ε_{vac}^{Ni} corresponding to $Ni_{23}Al_8$ for the 32 sites supercell. For noninteracting defects and sufficiently low concentrations of defects the energies ε_A^λ are independent of the concentration. The defect systems should also be at their ground states, i.e., no pressure is acting on them. This assumption can be lifted and more general expressions can be formulated including pressure-volume terms [56, 57].

Minimizing the grand canonical potential with respect to the number of point defects expressions for the concentrations of point defects are derived. For example, for a vacancy at a Ni site one obtains [57]

$$c_{vac}^{Ni} = \frac{M^{Ni}}{M} \frac{e^{-(\varepsilon_{vac}^{Ni} + \mu_{Ni})/kT}}{1 + e^{-(\varepsilon_{vac}^{Ni} + \mu_{Ni})/kT} + e^{-(\varepsilon_{Al}^{Ni} + \mu_{Ni} - \mu_{Al})/kT}} \tag{14}$$

where M represents the total number of available sites, and M^{Ni} the available sites of the Ni sublattice of Ni_3Al. In a similar way, the concentration for an antisite defect (Al atom on a Ni site) is expressed by

$$c_{Al}^{Ni} = \frac{M^{Ni}}{M} \frac{e^{-(\varepsilon_{Al}^{Ni} + \mu_{Ni} - \mu_{Al})/kT}}{1 + e^{-(\varepsilon_{vac}^{Ni} + \mu_{Ni})/kT} + e^{-(\varepsilon_{Al}^{Ni} + \mu_{Ni} - \mu_{Al})/kT}} \tag{15}$$

The concentrations for the Ni-rich defects (Al vacancy and Ni antisite) are formulated correspondingly. The so far unknown chemical potentials obey the equation

$$G = \mu_{Ni} N_{Ni} + \mu_{Al} N_{Al} \tag{16}$$

for the Gibbs energy G.

The general composition of the compound including the defects in a suitable way is given by $N_{Ni}/N_{Al} = x/(1 - x)$ where N_i is the total number of atomic species $i = \{Ni, Al\}$, and x varies in a small range around $x_0 = 0.75$ for Ni_3Al. With all the equations and conditions and including the supercell energy for the perfect compound the chemical potentials are calculated from a set of coupled equations. As is visualized by Equations 14 and 15 the defects are intermixed in order to maintain the overall composition. The chemical potentials depend on (p, T, x) in general. For example, the energy cost for the formation of a Ni vacancy for a given concentration x amounts to $E_{vac}^{Ni} = \varepsilon_{vac}^{Ni} + \mu_{Ni}(x)$. The chemical potential μ_{Ni} is the energy of adding a Ni atom. The discussed techniques were applied for example to Ni_3Al which is also well studied in literature [58].

The calculation of the *ab initio* energetics of a 32-atom supercell with a defect needs typically a few hours on a 2 GHz single-processor PC for a sufficient number of **k** points. This includes relaxation of the atomic positions which is now necessary because the defect destroys the $L1_2$ symmetry of the perfect Ni_3Al compound. For Ni_3Al the relaxation energy $\Delta\varepsilon(relax)$ as well as geometrical changes around the defect are largest when Al is placed at a position with other Al atoms as nearest neighbours, which is the case for an Al antisite atom on a Ni-sublattice site. Because the bond lengths in Ni_3Al are smaller by the considerable amount of 13% as compared to Al-Al distances in the free metal, Al in the compound tries to push neighbouring Al atoms away. This leads to an energy gain value of $\Delta\varepsilon(relax) = \varepsilon_{Al}^{Ni}(relax) - \varepsilon_{Al}^{Ni}(unrel) = -0.3$ eV applying directly the *ab initio* energies ε. A very strong size effect is even found for Al_3Ni [57]: the formation energy of a Ni vacancy is lower (more binding) than for an Al antisite. Usually, as it is also the case for Ni_3Al, antisite formation is less costly than the creation of vacancies.

For the *ab initio* set of the four defect formation energies (the Ni- and Al-vacancies, and the Ni- and Al-antisites) the statistical model yields the thermodynamical formation energies at 1000 K for the relaxed atomic positions, $E_{Al}^{Ni} = E_{Ni}^{Al} = 0.57$ eV, $E_{vac}^{Ni} = 1.51$ eV, $E_{vac}^{Al} = 2.0$ eV [59]. These results were obtained for the stoichiometric composition of $N_{Ni}/N_{Al} = 3/1$. Meaningful results for varying compositions can also be derived as long as the deviation from the 3/1 composition is sufficiently small, i.e., the defects can be considered to be noninteracting.

The antisite defects are the most probable defects because the energy cost is the lowest. The energies for both antisites in the grandcanonical formalism are equal because of the condition $N_{Ni}/N_{Al} = 3/1$. If the concentration changes, then the vacancy energies will be also involved, as the proper mixture of defects for a given global stoichiometry is governed by the chemical potentials μ_{Ni} and μ_{Al}.

Fig. 5 shows the calculated concentrations according to Equations 14 and 15. It should be noted that the absolute values of the concentrations are not to be taken too seriously due to the approximations of the statistical

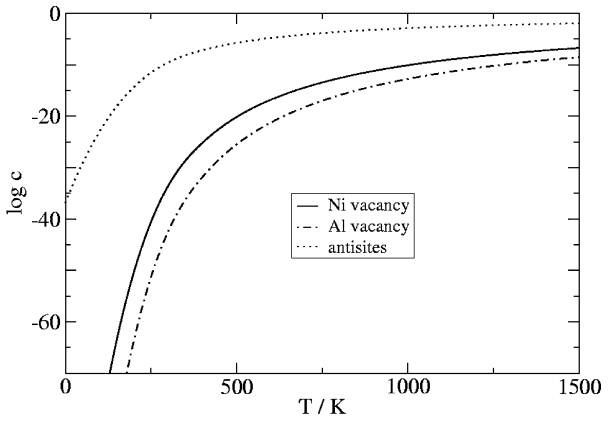

Figure 5 Point defect concentrations in Ni_3Al as calculated by a 32-atom supercell *ab initio* calculation.

model [57]. The relative concentrations, however, are meaningful. As is evident from Fig. 5 the concentration of antisites is by far the largest as follows from the low formation energies. Concerning the formation of vacancies, Ni vacancies are more abundant than Al vacancies by a factor of about 1000.

All atom jumps observed e.g., during resistivity relaxation experiments in Ni_3Al are assumed to take place by exchange with vacancies. Studying possible processes for creating disorder such as Al jumps to a vacant Ni site and vice versa (Fig. 6a and b) calculations were done for the paths by displacing the migrating atom in a quasi-static way and partially relaxing the positions of the surrounding atoms (full lines in Fig. 6a and b). Not relaxing the atoms, i.e., freezing the lattice, results in significantly higher energy barriers (dashed lines in the figure). Because Ni vacancies are easier to form ($E_{\mathrm{vac}}^{\mathrm{Ni}} = 1.51$ eV) than Al vacancies ($E_{\mathrm{vac}}^{\mathrm{Al}} = 2.0$ eV) the most probable creation of disorder is moving an Al atom to a vacant Ni site (Fig. 6a). The energy profile shows a striking asymmetry: The barrier for the forward jump is about 1.0 eV, much larger than 0.3 eV for the back jump. This is due to the fact that after jumping to a Ni site Al has now three nearest neighbour Al atoms. This situation is energetically unfavourable because of

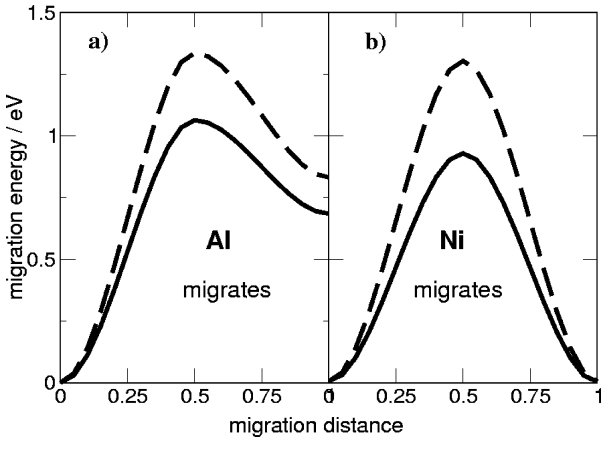

Figure 6 Energy profiles for migration of a single Al atom towards a Ni vacancy (panel a) and a single Ni atom towards an Al vacancy (panel b) for Ni_3Al. Dashed line: unrelaxed atomic positions; full line: positions relaxed.

the larger atomic radius of Al as compared to Ni. When Ni is jumping to an Al vacancy (Fig. 6b) the barrier is *symmetric*: Ni easily fits into the vacant Al site. In other words the energy for a single Al vacancy is practically the same as for the combined defect of a Ni antisite with a neighbouring Ni vacancy.

5. Interpretation of REST measurements by MC and *ab initio* calculations: Ideal picture and practical puzzles

The signal obtained from a resistivity measurement contains a multitude of microscopic contributions which add up in an intricate, highly complex manner. If we want a reasonable interpretation of the macroscopic data in terms of atom jumps, we must re-enact this statistical co-operation and interconnection in a theoretical model. This can be done in a hierarchy of steps. On the lowest level, the transition probability of the single atom jump in a given atomic environment can be calculated by a suitable *ab initio* or molecular dynamics method. Next, the crystal structure defines the jump geometry, which for the intermetallic compounds considered here is given by the positions of the nearest neighbour atoms adjacent to the vacancy. Next, a kinetic MC algorithm sums up the single atom jumps statistically. The resulting configuration must then be described by the proper parameters which enter electrical resistivity theory, for instance LRO and SRO parameters. The kinetic rates of these parameters can then be analysed in a similar way as the kinetic rates from experiment. For example, we can make an activation analysis by an Arrhenius plot and investigate how the integral parameters obtained thereof relate to the single atom jump processes.

A combined attack along similar lines has recently been tried on Ni_3Al as a model system. Order-order relaxation kinetics was first studied by means of high precision resistometry. Then atomic jump processes were modeled by Monte Carlo simulations and finally defect energies were calculated by *ab initio* methods. Measurements gave evidence for the simultaneous action of two exponential thermally activated processes with a comparatively high activation energy greater than 4 eV [23, 24]. The same qualitative scenario followed from MC simulations using a Glauber algorithm with plausible interaction energies as input which correspond to the order-disorder transition. The faster process could be identified as the fast annihilation/production of antisite pairs, whereas the much slower second process was interpreted as mainly due to the separation and distribution of antisites [40]. Looking for microscopic reasons for the rapid creation of antisite pairs, migration profiles of atoms were calculated by the *ab initio* methods described above and in fact led to a striking result. As shown in Fig. 6 an Al atom jumping to a Ni site ends up in a very shallow energy minimum at higher energy level which results in a much larger probability for jumping back than for reaching the antisite position. How can Al antisite defects which are needed to create disorder then be stabilised? A very convincing mechanism is to assume that the back jump of Al is blocked by a practically simultaneous migration of a Ni atom

towards the just created Al vacancy. We calculated barriers for such co-operative jumps by studying moving pairs of Ni and Al atoms. The smallest barriers for such jumps with a symmetric energy profile are in the order of 1.5 eV (in a relaxed atom environment), which is larger but still comparable to the barrier of the single-atom Al jump. Therefore, a reasonable finite probability exists that the empty Al site is indeed blocked and Al can remain in its antisite position. Similar results have very recently been found by molecular dynamics simulation [60] showing a considerable increase in barrier height in comparison to molecular statics calculations. This is a further strong indication for a co-operative coupling of atom jumps.

Estimating the overall activation energy for the change of order, i.e., the energy derived from the residual resistivity measurements, we add the largest vacancy formation energy and a barrier height of about 1.5 eV resulting in a value not larger than 3.5 eV which is in some disagreement with the experimentally determined value lying above 4 eV. We have to keep in mind, however, the speed of the transition. If its time scale is considerably shorter than that for relaxation of the surrounding lattice sites a higher barrier can ensue. The calculated antisite energies on the other hand fit very well to data determined by a statistical-thermodynamic model from activity measurements [61]. At present we try to resolve the discrepancy by using Ni_3Al specimens without boron additions. Also single crystal samples will be used. Experiments are being extended to other $L1_2$-ordered compounds, e.g., Ni_3Ga, and other ordering systems, e.g., B2-ordered FeAl and $L1_0$-ordered FePd. Further, the partially inadequate Glauber algorithm is presently replaced by a residence time algorithm which is expected to yield a realistic Arrhenius behaviour of the kinetic processes. Jump barriers based on *ab initio* results and depending on the specific atomic environment of the jumping atom are to be incorporated into the MC algorithm.

The primary aim of the combined application of the methods we have just described is thus to make sure what is really contained in the macroscopic experimental signal like resisitivity or heat transfer, enabling therefore a valid interpretation. However, we want to draw attention to the fact that simulation gives a wealth of structural and kinetic information on a continuous sequence of scales beginning from the co-operation of single atoms. This is of great help in unravelling the details of complex combined reactions (e.g., Fig. 4) where the integrating measurement leaves open several possibilities of explanation. Tracking the behaviour of the diffusion-mediating defect can provide insight on otherwise puzzling results, such as when the character of a phase transformation deviates strongly from what is expected ín the light of continuum theories [22].

In conclusion, the application of modern *ab initio* techniques allows a detailed study of the energetics of atom interaction with reliable numerical results. However, for a complete description of the actual defect formation, migration and annihilation, and to connect the macroscopic kinetic observables to their microscopic constituents, Monte Carlo simulations are the methods of choice, with the transition probabilities for atom jumps based on density functional *ab initio* results. We believe that the combination of judiciously chosen, highly sensitive experiments, up-to-date *ab initio* calculations and Monte Carlo techniques is a powerful set of tools to gain a fundamental understanding of the role of defects in compounds, which will allow to answer open questions on configurational kinetics in a truly quantitative manner.

References

1. J. H. WESTBROOK and R. L. FLEISCHER, in "Intermetallic Compounds-Principles and Practice" (Wiley, Chichester, 1994) Vols. 1 and 2.
2. G. SAUTHOFF, "Intermetallics" (VCH Verlagsgesellschaft, Weinheim, 1995).
3. C. YANAR, J. M. K. WIEZOREK and W. A. SOFFA, in "Phase Transformations and Evolution in Materials," edited by E. A. Turchi and A. Gonis (The Minerals, Metals & Materials Society, Warrendale, 2000) p. 39.
4. M. E. McHENRY and D. E. LAUGHLIN, *Acta Mater.* **48** (2000) 223.
5. K. TANAKA and K. MORIOKA, *Phil. Mag.* **A**, in press.
6. K. MORIOKA and K. TANAKA, in Proceedings of the 4th Pacific Rim International Conference on Advanced Materials and Processing (PRICM4), edited by S. Hanada, Z. Zong, S. H. Nam and R. N. Wright (The Japan Institute of Metals, Sendai, 2001) p. 1703.
7. ST. FRANK, U. SÖDERVALL and CHR. HERZIG, *Intermetallics* **5** (1997) 221.
8. S. V. DIVINSKI, ST. FRANK, U. SÖDERVALL and CHR. HERZIG, *Acta Mater.* **46** (1998) 4369.
9. ST. FRANK, U. SÖDERVALL and CHR. HERZIG, *Phys. Stat. Sol.* B **191** (1995) 45.
10. ST. FRANK, S.V. DIVINSKI, U. SÖDERVALL and CHR. HERZIG, *Acta Mater.* **49** (2001) 1399.
11. H. THIESS, M. KAISERMAYR, B. SEPIOL, M. SLADECEK, R. RÜFFER and G. VOGL, *Phys. Rev.* B **64** (2001) 104305.
12. B. SEPIOL, A. MEYER, G. VOGL, H. FRANZ and R. RÜFFER, *ibid.* B **57** (1998) 10433.
13. W. PFEILER and B. SPRUSIL, *Mater. Sci. Eng.* A **324** (2002) 34.
14. W. PFEILER, *JOM* **52** (2000) 14.
15. *Idem.*, in "Properties of Complex Inorganic Solids," edited by A. Gonis, A. Meike and E. A. Turchi (Plenum Press, New York, 1997) p. 219.
16. J. C. DESOYER, P. GROSBRAS and P. MOINE, in "Solid State Phase Transformations in Metals and Alloys," edited by D. de Fontaine (Les Éditions de Physique, Paris, 1980) p.197.
17. P. L. ROSSITER, "The Electrical Resistivity of Metals and Alloys" (Cambridge University Press, Cambridge, 1987) p. 160ff.
18. H. LANG, T. MOHRI and W. PFEILER, *Intermetallics* **7** (1999) 1373.
19. H. LANG, H. UZAWA, T. MOHRI and W. PFEILER, *ibid.* **9** (2001) 9.
20. A. KULOVITS, W. A. SOFFA, W. PÜSCHL and W. PFEILER, *Mater. Res. Soc. Symp. Proc.* **753** (2003) BB5.37.
21. H. LANG, K. ROHRHOFER, P. ROSENKRANZ, R. KOZUBSKI, W. PÜSCHL and W. PFEILER, *Intermetallics* **10** (2002) 283.
22. W. A. SOFFA, W. PÜSCHL and W. PFEILER, *ibid.* **11** (2003) 161.
23. R. KOZUBSKI and W. PFEILER, *Acta Mater.* **44** (1996) 1573.
24. R. KOZUBSKI, *Progr. Mater. Sci.* **41** (1997) 1.
25. K. D. BELASHENKO and V. G. VAKS, *J. Phys.: Cond. Matter* **10** (1998) 1965.
26. V. G. VAKS, S. V. BEIDEN and V. YU. DOBRETSOV, *JETP Lett.* **61** (1995) 68.

27. V. G. VAKS, *ibid.* **63** (1996) 471.
28. K. BINDER and D. W. HEERMANN, "Monte Carlo Simulation in Statistical Physics," 3rd ed. (Springer, Berlin-Heidelberg, 1997).
29. N. METROPOLIS, A. W. ROSENBLUTH, M. N. ROSENBLUTH, A.H. TELLER, and E. TELLER, *J. Chem. Phys.* **21** (1953) 1087.
30. R. J. GLAUBER, *J. Math. Phys.* **4** (1963) 294.
31. W. M. YOUNG and E. ELCOCK, *Proc. Phys. Soc.* **89** (1966) 735.
32. A. B. BÖRTZ, M. H. KALOS and J. L. LEBOWITZ, *J. Comp. Phys.* **17** (1975) 10.
33. F. HAIDER, in "Ordering and Disordering in Alloys," edited by R. Yavari (Elsevier Applied Science, Londion and New York, 1993) p. 215.
34. G. H VINEYARD, *J. Phys. Chem. Solids* **3** (1957) 121.
35. T. F. LINDSEY and B. FULTZ, in "Diffusion in Ordered Alloys," edited by B. Fultz, R. W. Cahn and D. Gupta (The Minerals, Metals and Materials Society, 1993) p. 91.
36. B. FULTZ, *J. Chem. Phys.* **88**(1988) 3227.
37. U. GAHN and W. PITSCH, *Z. Metallk.* **78** (1987) 324.
38. *Idem., Acta Metall.* **37** (1989) 2455.
39. P. ORAMUS, R. KOZUBSKI, V. PIERRON-BOHNES, M. C. CADEVILLE, C. MASSOBRIO and W. PFEILER, *Mater. Sci. Eng.* A **324** (2002) 11.
40. P. ORAMUS, R. KOZUBSKI, V. PIERRON-BOHNES, M. C. CADEVILLE and W. PFEILER, *Phys. Rev.* B **63** (2001) 174109.
41. R. KOZUBSKI, P. ORAMUS, W. PFEILER,V. PIERRON-BOHNES and M. C. CADEVILLE, in Proceedings Solid-Solid phase transformations '99 (JIMIC-3) edited by M. Koiwa, K. Otsuka and T. Miyazaki (The Japan Insitute of Metals, 1999) p. 473.
42. M. ATHÈNES, P. BELLON, G. MARTIN and F. HAIDER, *Acta Mater.* **44** (1996) 4739.
43. K. OKI, H. SAGANE and T. EGUCHI, *J. de Physique (Paris) Colloq.* **38** (1977) C7-414.
44. S. M. ALLEN and J. W. CAHN, *Acta Metall.* **24** (1976) 425.
45. P. FRATZL and O. PENROSE, *Acta Metall. Mater.* **43** (1995) 2921.
46. C. A. LABERGE, P. FRATZL and J. L. LEBOWITZ, *Phys. Rev. Lett.* **75** (1995) 4448.
47. P. FRATZL and O. PENROSE, *Phys. Rev.* B **55** (1997) R6101.
48. M. ATHÈNES, P. BELLON and G. MARTIN, *Phil. Mag.* A **76** (1997) 527.
49. H. HOHENBERG and W. KOHN, *Phys. Rev.* B **136** (1964) 864.
50. W. KOHN and L. SHAM, *ibid.* A **140** (1965) 1133.
51. R. PODLOUCKY, R. ZELLER and P. H. DEDERICHS, *ibid.* B **22** (1980) 5777.
52. N. PAPANIKOLAOU, R. ZELLER, P. H. DEDERICHS and N. STEFANOU, *ibid.* B **55** (1997) 1157.
53. H. KRAKAUER, M. POSTERNAK and A. J. FREEMAN, *ibid.* B **19** (1979) 1706; E. Wimmer, M. Weinert and A. J. Freeman, *ibid.* B **24** (1981) 864.
54. P. BLÖCHL, *ibid.* B **50** (1994) 17953.
55. G. KRESSE and J. HAFNER. *Phys. Rev.* B **48** (1993) 13115; B **49** (1994) 14251; G. Kresse and J. Furthmüller, *Comput. Mater. Sci.* **6** (1996) 15; *Phys. Rev.* B **54** (1996) 11169.
56. B. MEYER and M. FÄHNLE, *Phys. Rev.* B **59** (1991) 6072; *Phys. Rev.* B **60** (1999) 717.
57. M. RASAMNY, M. WEINERT, G. W. FERNANDO and R. E. WATSON, *ibid.* B **64** (2001) 144107.
58. S. M. FOILES and M. S. DAW, *J. Mater. Res.* **2** (1987) 5; S. B. DEBIAGGI, P. M. DECORTE and A. M. MONTI, *Phys. Stat. Sol.* (b) **195** (1996) 37; F. GAO, D. J. BACON and G. J. ACKLAND, *Phil. Mag.* A **67** (1993) 275; C. L. FU and G. S. PAINTER, *Acta Mater.* **45** (1997) 481.
59. H. SCHWEIGER, R. PODLOUCKY, W. PÜSCHL and W. PFEILER, *Mater. Res. Soc. Symp. Proc.* **646** (2001) N5.11.1.
60. P. ORAMUS, C. MASSOBRIO, M. KOZŁOWSKI, R. KOZUBSKI, V. PIERRON-BOHNES, M.C. CADEVILLE and W. PFEILER, *Compu. Mater. Sci.* **27** (2003) 186.
61. H. SCHWEIGER, G. SEMENOVA, W. WOLF, W. PÜSCHL, W. PFEILER, R. PODLOUCKY and H. IPSER, *Scripta Mater* **46** (2002) 36.